SMC-TR-98-13

AEROSPACE REPORT NO.
TR-93(3935)-15

Failure Modes of a Unidirectional Ultra-High-Modulus Carbon-Fiber/Carbon-Matrix Composite

15 January 1998

Prepared by

R. J. ZALDIVAR and G. S. RELLICK
Mechanics and Materials Technology Center
Technology Operations

J-M Yang
Department of Materials Science and Engineering
University of California, Los Angeles

Prepared for

SPACE AND MISSILE SYSTEMS CENTER
AIR FORCE MATERIEL COMMAND
2430 E. El Segundo Boulevard
Los Angeles Air Force Base, CA 90245

Engineering and Technology Group

19980708 003

THE AEROSPACE CORPORATION
El Segundo, California

APPROVED FOR PUBLIC RELEASE;
DISTRIBUTION UNLIMITED

This report was submitted by The Aerospace Corporation, El Segundo, CA 90245-4691, under Contract No. F04701-93-C-0094 with the Space and Missile Systems Center, 2430 E. El Segundo Blvd., Los Angeles Air Force Base, CA 90245. It was reviewed and approved for The Aerospace Corporation by S. Feuerstein Principal Director, Mechanics and Materials Technology Center. Maj. J. W. Cole was the project officer for the Mission-Oriented Investigation and Experimentation (MOIE) program.

This report has been reviewed by the Public Affairs Office (PAS) and is releasable to the National Technical Information Service (NTIS). At NTIS, it will be available to the general public, including foreign nationals.

This technical report has been reviewed and is approved for publication. Publication of this report does not constitute Air Force approval of the report's findings or conclusions. It is published only for the exchange and stimulation of ideas.

MAJ. J. W. COLE
SMC/AXES

REPORT DOCUMENTATION PAGE

Form Approved
OMB No. 0704-0188

Public reporting burden for this collection of information is estimated to average 1 hour per response, including the time for reviewing instructions, searching existing data sources, gathering and maintaining the data needed, and completing and reviewing the collection of information. Send comments regarding this burden estimate or any other aspect of this collection of information, including suggestions for reducing this burden to Washington Headquarters Services, Directorate for Information Operations and Reports, 1215 Jefferson Davis Highway, Suite 1204, Arlington, VA 22202-4302, and to the Office of Management and Budget, Paperwork Reduction Project (0704-0188), Washington, DC 20503.

1. AGENCY USE ONLY (Leave blank)	2. REPORT DATE	3. REPORT TYPE AND DATES COVERED
	15 January 1997	

4. TITLE AND SUBTITLE
Failure Modes of a Unidirectional Ultra-High-Modulus Carbon-Fiber/Carbon-Matrix Composite

5. FUNDING NUMBERS
F04701-93-C-0094

6. AUTHOR(S)
R. J. Zaldivar, G. S. Rellick, and J-M Yang

7. PERFORMING ORGANIZATION NAME(S) AND ADDRESS(ES)
The Aerospace Corporation
Technology Operations
El Segundo, CA 90245

8. PERFORMING ORGANIZATION REPORT NUMBER
TR-93(3935)-15

9. SPONSORING/MONITORING AGENCY NAME(S) AND ADDRESS(ES)
Space and Missile Systems Center
Air Force Materiel Command
2430 E. El Segundo Blvd.
Los Angeles Air Force Base, CA 90245

10. SPONSORING/MONITORING AGENCY REPORT NUMBER
SMC-TR-98-13

11. SUPPLEMENTARY NOTES

12a. DISTRIBUTION/AVAILABILITY STATEMENT
Approved for public release; distribution unlimited

12b. DISTRIBUTION CODE

13. ABSTRACT (Maximum 200 words)

The objective of this study was to observe the effects of various microstructural features on the in situ, room-temperature tensile fracture behavior of an ultra-high-modulus, unidirectional carbon/carbon (C/C) composite as a function of processing heat-treatment temperature (HTT) over the range of 1100°C to 2750°C. An in situ SEM flexural stage was used to observe the interactions between the advancing crack tip and the microstructural features in the frontal process zone. Following the lowest HTT of 1100°C, failure is dominated by the well-bounded brittle matrix; a tortuous crack path in the E130 fibers appears to contribute to a relatively high utilization of fiber strength in spite of this brittle-matrix failure. Approximate calculations of the interfacial shear stress that might be generated by matrix shrinkage during pyrolysis of the polymer to carbon were compared to approximations of crack-tip interfacial shear stresses (IFSS) using the Cook-Gordon approach. The results suggest that the strong bonding in the 1100°C HTT composite cannot be accounted for by friction alone, and, therefore, chemical bonding or some type of fiber-matrix mechanical interlocking must be involved. Higher HHTs lead to progressive weakening of the fiber-matrix interface, and, with heat treatment to 2150°C, multiple matrix cracking (MMC) is observed. Using the crack-spacing model of Aveston, Cooper, and Kelly (ACK), an IFSS of 1 MPa is estimated for the MMC case. Attempts to calculate the matrix failure strain using the ACK formulation led to a large overprediction of the failure strain, although a number of the parameters used in the calculation are known only very approximately. Heat treatments to 2400°C and 2750°C led to longitudinal intramatrix cohesive failure; at 2750°C, this damage is extensive and results in composites with strength utilizations approaching those of dry fiber bundles.

14. SUBJECT TERMS
Composites, Carbon-carbon, Carbon fibers

15. NUMBER OF PAGES
10

16. PRICE CODE

17. SECURITY CLASSIFICATION OF REPORT	18. SECURITY CLASSIFICATION OF THIS PAGE	19. SECURITY CLASSIFICATION OF ABSTRACT	20. LIMITATION OF ABSTRACT
UNCLASSIFIED	UNCLASSIFIED	UNCLASSIFIED	

DTIC QUALITY INSPECTED 1

Contents

I. Introduction 1

II. Experimental Procedure 2

III. Results 3

IV. Discussion 7

V. Conclusions 9

APPENDIX 9

References 10

Figures

1. Schematic diagram of experimental arrangement for *in situ* flexure testing 2

2. Brittle fracture of composite heat-treated to 1100°C 2

3. View of crack propagation in E130 composite prior to crack opening revealing intrafilament crack deflection 3

4. Fracture behavior of E130 composite heat-treated to 1600°C exhibiting mixed mode failure 3

5. High-magnification micrograph showing crack blunting in interfacial region of 2150°C heat-treated composite 4

6. Matrix crack bridged by intact fibers (2150°C HTT) 4

7. Multiple matrix cracks formed in 2150°C heat-treated composite 4

8. Matrix slippage over bridging fibers in 2150°C heat-treated composite 5

9. High-magnification micrograph showing crack blunting at graphitized matrix sheath structure in 2400°C heat-treated composite 5

10. Short-range longitudinal intramatrix splitting in 2400°C heat-treated composite 5

11. Crack propagation through a 2400°C heat-treated composite at three levels of strain 6

12. Crack zone showing well-defined regions of nongraphitized matrix, graphitized sheath, and fiber in 2400°C heat-treated composite 7

13. Crack propagation through a 2750°C heat-treated composite at two different degrees of strain 8

Tables

I. Fiber Strength Utilization (FSU) for the Different Composites by HTT 1

I. Introduction

BECAUSE of the very low failure strains of most carbon matrices, carbon-fiber/carbon-matrix composites—so-called carbon/carbon (C/C)—fall into the category of brittle-matrix composites. Nevertheless, in spite of extensive interest in the fracture behavior of uniaxially fiber-reinforced ceramic-matrix composites,[1] there have been few efforts to study in detail the microstructural characteristics involved in the fracture behavior of similarly constructed C/Cs.[2-5] Rather, more attention has been directed to 2D reinforced cloth laminate C/Cs,[6-10] including, recently, a 2D SiC-fiber-reinforced carbon matrix.[11] While such studies have provided useful insights into the mechanical behavior of different types of C/Cs under a variety of conditions, the complicated microstructures of carbon systems have made it extremely difficult to isolate the effects of specific microstructural features in the fracture process.

In this current investigation, we expand on earlier work[12] in which we measured the *in situ* fiber strength utilization (FSU) as a function of heat-treatment temperature (HTT) for a series of unidirectional C/Cs fabricated from four Du Pont mesophase-derived carbon fibers and a poly(arylacetylene) (PAA) resin matrix precursor. FSU was defined as the ratio of apparent fiber strength in the C/C to the fiber strength in an epoxy-resin-matrix composite. The problem of low FSU in C/C has been noted for many years, beginning with the work of Fitzer and Burger[2] on carbonized unidirectional composites, followed by Newling and Walker,[3] and then by Thomas and Walker,[13] who invoked the Cook–Gordon[14] mechanism of toughening of brittle solids to explain the improved FSU of C/Cs at higher HTTs.

In the earlier work we cited,[12] the FSUs of the E35, E75, E105, and E130 fiber†/PAA composites (where the number in the fiber designation is the fiber tensile modulus in units of Mpsi) were studied as a function of five processing conditions: the cured-resin composite, and HTTs of 1100°, 2150°, 2400°, and 2750°C. The results are summarized in Table I to illustrate the wide differences in FSU among this family of fibers, all of which are derived from the same mesophase precursor.

Following the HTT of 1100°C (carbonization), the E35, E75, and E105 C/C composites experienced large reductions in failure strain (~0.1–0.2%) and, hence, in FSU (24–35%), relative to the same fibers in the baseline epoxy-matrix composites. In contrast, the E130 composite had an FSU of 79%.

Scanning electron micrographs (SEMs) of the fracture surfaces revealed that the three lower-modulus fiber composites experienced matrix-dominated brittle fracture; i.e., crack-tip stresses at the fiber–matrix interface were sufficiently high to fracture the fibers, leading to a smooth fracture surface with no

Table I. Fiber Strength Utilization (FSU) for the Different Composites by HTT†

Fiber	Cured resin	FSU (%)			
		1100°C	2150°C	2400°C	2750°C
E35	100	24	28	60	31
E75	100	24	62	74	28
E105	100	35	72	74	34
E130	100	79	92	68	42

†From Ref. 12.

†A series of experimental carbon fibers from Du Pont derived from mesophase pitch.

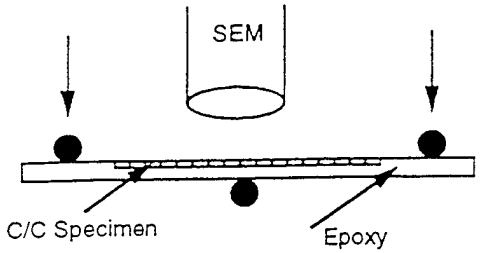

Fig. 1. Schematic diagram of experimental arrangement for *in situ* flexure testing.

fiber pullout. The E130 fiber composite revealed a rougher fracture surface with distinct, but limited, fiber pullout. The striking characteristic, however, of the E130 composite was the very jagged, rough fracture of the E130 filaments themselves; this fiber microstructure was believed to be the major factor contributing to the composite toughness and improved yield of fiber strength relative to the other three composites. Another factor that may come into play in the E130 composite is a reduced interfacial bond strength owing to the low chemical activity of highly oriented, ultra-high-modulus fibers such as E130. While the debate over chemical versus frictional bonding in C/C is far from resolved, recent transmission electron microscopy (TEM) studies[15] have revealed examples of intimate fusion between fiber and matrix in high-HTT (>2000°C) composites. However, such bonding in C/Cs may be only the remnants of bonding in the earlier stages of C/C processing—specifically during the degradation/pyrolysis of the polymer-matrix precursor. Such bonding would presumably be a factor in the development of residual compressive radial stresses at the fiber–matrix interface, thereby affecting the composite fracture behavior through the frictional interfacial shear strength.

With heat treatment to 2150°, 2400°, and 2750°C we observed in all four composites a "recovery" of fiber strength for HTT to 2150° or 2400°C. This is principally the result of an interface weakening, as inferred by significant fiber pullout in the specimen fracture surfaces; the weaker interface works to overcome matrix-dominated composite failure. With heat treatment to 2750°C, all the composites experienced significant reductions in FSU. For this HTT, SEM micrographs showed evidence of fiber degradation in the lower form of longitudinal fiber splitting.[12] This damage was believed to be a consequence of the composite thermal stresses induced by this high HTT since the fibers when heat-treated alone to 2750°C showed strength increases.

The objective of this current paper is to report, in detail, results from an investigation of the failure mechanisms of one of these composites, the E130 C/C, as a function of HTT using an SEM flexure stage. We were particularly interested in the behavior of the crack tip as it advanced through the various composite microstructural elements.

II. Experimental Procedure

Unidirectional composites were fabricated by solution impregnation of PAA/methyl ethyl ketone into single tows of the E130 mesophase-pitch-derived carbon fibers. Each tow contained 3000 filaments. The single-tow composites were then air-dried and cured at 250°C. Subsequent heat treatments were performed at 1100°, 1600°, 2150°, 2400°, and 2750°C for 1 h in argon. More complete details of the composite tensile testing can be found in Ref. 12. Discussions of the PAA resin matrix precursor have also been reported elsewhere,[16,17] as have the fiber volume fractions V_f of these same composites.[18] In the cured state, V_f was found to be about 0.20. Upon carbonization (1100°C), consolidation of the composite resulted in V_f increasing to a nominal value of 0.30. This value remained essentially constant with further heat treatment through 2400°C.

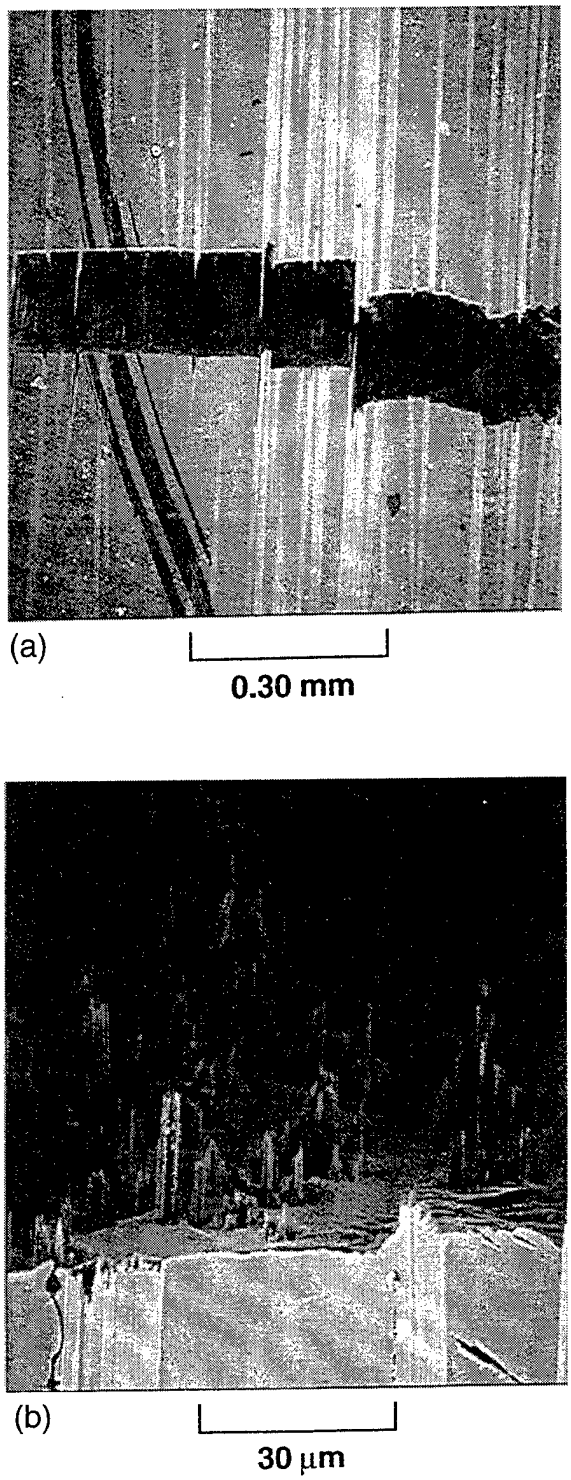

Fig. 2. Brittle fracture of composite heat-treated to 1100°C: (a) low magnification, (b) higher magnification revealing jagged filament fracture.

Because of the small size of the tow composites (~1 mm diameter), they were mounted in epoxy resin, then polished to an optical finish. The specimens were oriented so that the fibers were aligned in the direction of the applied tension. A xenon-ion etching procedure was also performed on the specimens to enhance the distinction between carbon microstructures.[19,20] Excess mounting resin was machined away, leaving the C/C specimen embedded in the minimum amount of resin. The advantages of having the epoxy support are twofold: First, it avoids crushing damage to the specimen at the loading pins since the load is applied directly to the epoxy; second, the

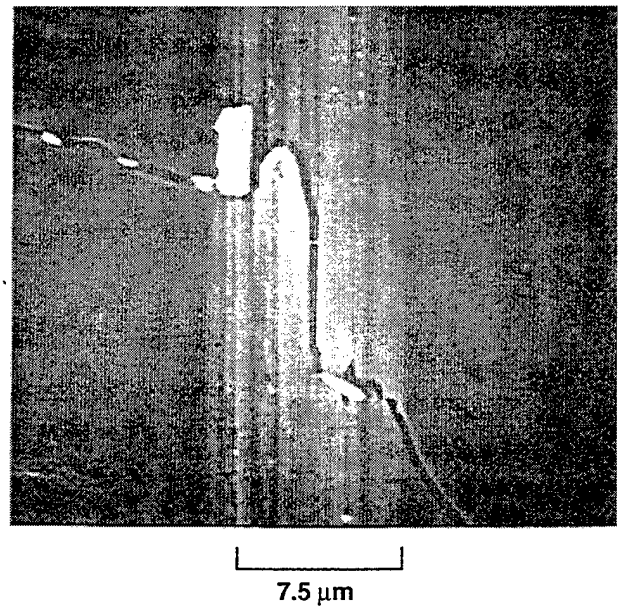

Fig. 3. View of crack propagation in E130 composite prior to crack opening revealing intrafilament crack deflection.

epoxy keeps the composite intact during the later stages of crack propagation. Figure 1 shows a schematic of the sample arrangement used for *in situ* SEM observations. The assembly was fitted with a displacement control loading mechanism that could be manually controlled from outside the SEM. The span-to-depth ratio of the samples was approximately 50:1 to ensure a close approximation of tensile failure at the surface. Observations were made on the exposed tensile face. Unfortunately, the stage was not equipped to measure either load or deflection with significant accuracy. Initially, efforts were made to introduce small matrix cracks with a Vickers indenter. However, the results of this approach were that in most cases the manufactured flaws did not initiate a steady-state matrix crack. This is the same observation made by Marshall and Evans[21] in their studies of the *in situ* failure behavior of a SiC/glass-ceramic composite. The best results were obtained by observing the polished specimen surface at a magnification sufficiently low to detect the first matrix crack, then focusing on this region at higher magnification as the displacement was progressively increased.

III. Results

Figures 2(a) and (b) show the fracture surface of an E130 composite heat-treated to 1100°C. A single matrix crack has propagated through the entire width of the composite (perpendicular to the load direction), fracturing both matrix and fibers. Figure 2(b) reveals that rather than the crack propagating directly through the filaments, as was the case for other E-type fibers in this same matrix,[12] there is a high degree of crack deflection *within* the E130 filaments. Figure 3 shows a high-magnification micrograph of a deflected crack (moving from left to right) within a filament at a point where the crack has not yet opened appreciably. This energy-absorbing fracture path through the filaments very likely contributes to the higher strength utilization of these composites over that of other E-type fiber composites (Table I), all of which experienced planar brittle failure of the fibers and gave significantly lower strength utilizations, consistent with matrix-dominated failure, i.e., composite failure occurring at the failure strain of the matrix. For example, the E75 and E105 composites heat-treated to 1100°C both failed at about 0.1% strain, whereas the E130 composite failed at about 0.2%. The absolute difference, of course, is small, but, we believe, significant. Interface weakening may also play a role in the higher failure strain and FSU of the E130 composite. For example, Edie *et al.*[22] found that the interlaminar shear strengths of these same four fibers in an epoxy matrix decreased monotonically with increasing fiber modulus.

For a HTT of 1600°C, we observed a mixed-mode failure (Figs. 4(a) and (b)); i.e., there was a combination of matrix-induced fiber failure as well as some interfacial crack deflection consistent with some local weakening, or even possibly debonding, of the fiber–matrix interface with HTT. This is illustrated well in Fig. 4(b), where we see one fiber that has failed at a distance of about 6 mm from the primary matrix crack. This fracture mode allows some of the intact fibers to bridge the crack, contributing to crack-tip shielding and leading to higher fiber strength utilizations. (Note: FSU was not measured for the 1600°C HTT.)

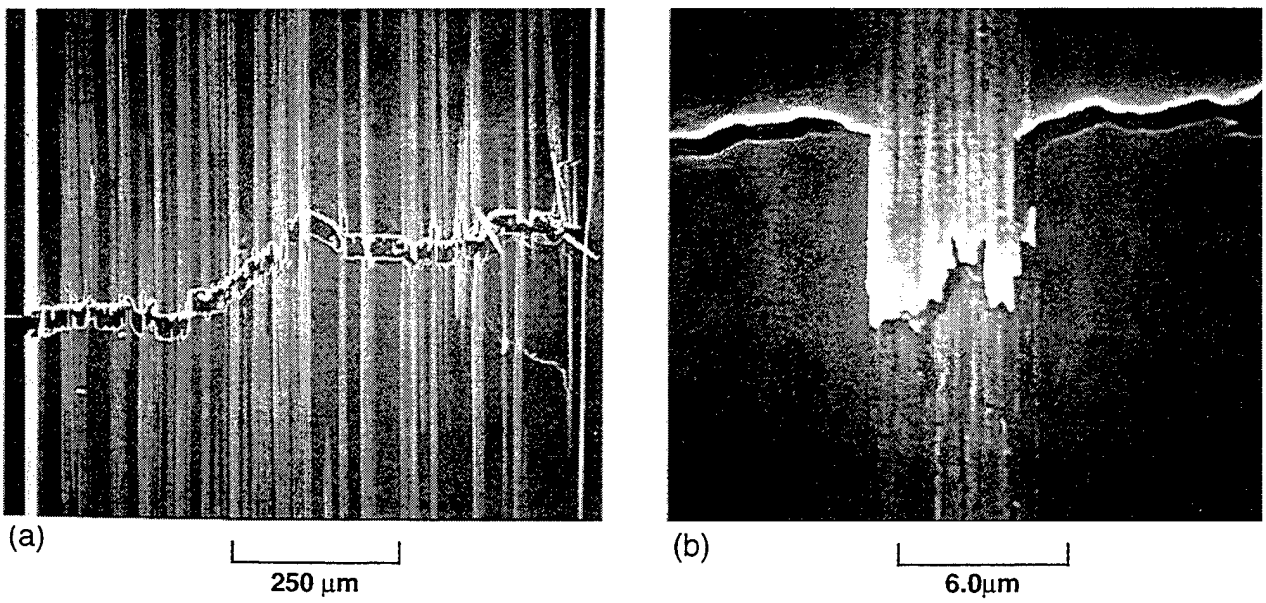

Fig. 4. Fracture behavior of E130 composite heat-treated to 1600°C exhibiting mixed mode failure: (a) low magnification, (b) higher magnification showing a filament break occurring about 6 mm from the matrix crack.

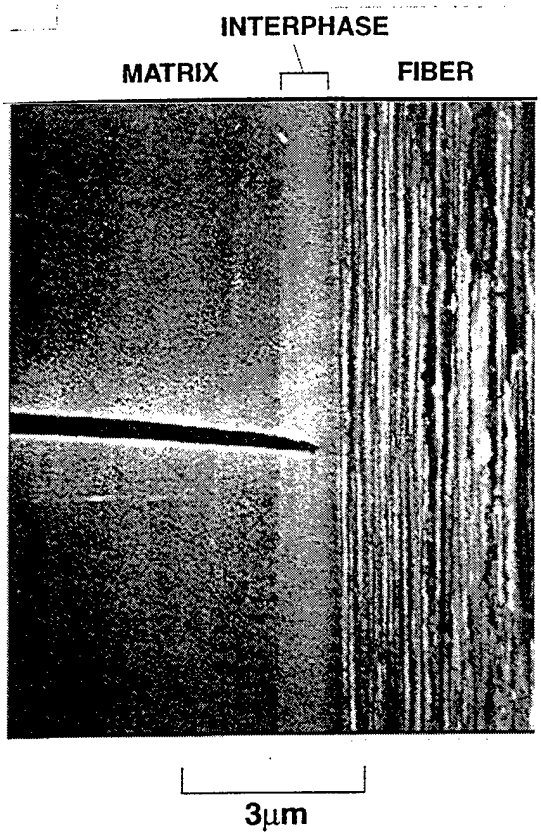

Fig. 5. High-magnification micrograph showing crack blunting in interfacial region of 2150°C heat-treated composite.

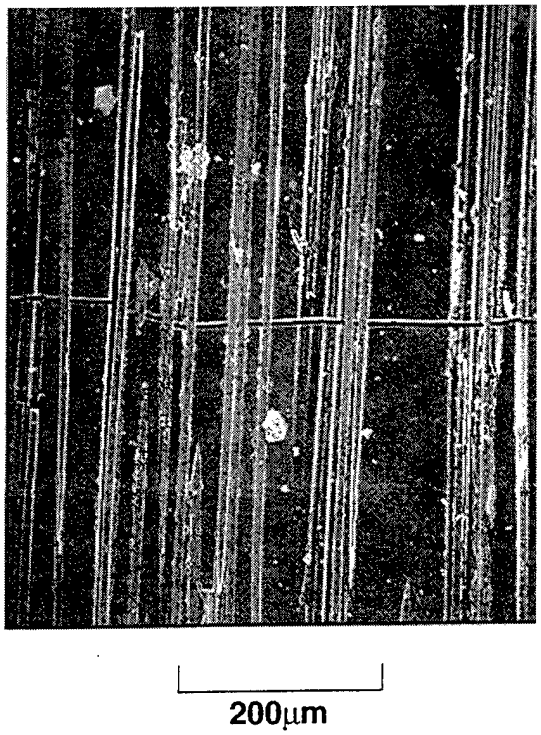

Fig. 6. Matrix crack bridged by intact fibers (2150°C HTT).

With heat treatment to 2150°C, we see the first clear evidence, at typical SEM magnifications, of a matrix interphase structure (Fig. 5). As discussed previously,[20] this interphase is a region of higher preferred orientation and enhanced crystalline development[15] as a consequence of matrix deformation during pyrolysis and carbonization. We have argued that the source of this deformation is the restraint of matrix shrinkage at the fiber surface resulting from attractive or frictional forces between fiber and matrix.[20] Independent measurements by TEM-selected area diffraction[15] of these same and similar composites have confirmed repeatedly that the zone of matrix around the fiber (from ~0.5 to 2.0 μm) is better graphitized and better oriented than the "bulk" matrix farther from the fibers. This is evident at HTTs as low as 1100°C.[15] For the case of the SEM of Fig. 5, the greater brightness of the sheath is most likely the result of its higher density,[18] which results in a higher electron emission. It is also possible that the contrast between interphase and "bulk" matrix is due to the differences in orientation. Also, because of the relatively low HTT of 2150°C, this matrix interphase "sheath"[23] structure is not well graphitized and, therefore, does not have the lamellar graphitic texture seen in the highly graphitized E130 fiber adjacent to it. This lamellar, or grooved, texture of etched graphite, as seen by standard secondary-electron images, is a consequence of topographic contrast. Whether due to ion bombardment or reactive etching, the less crystalline, more defective areas tend to erode more, leaving a topography of "hills and valleys."

Composites heat-treated to 2150°C no longer experienced matrix-dominated failure. Matrix cracks that form on the composite surface can apparently be blunted at the interphase region, as illustrated in Fig. 5. However, the orientation and graphitization of the interphase is not sufficiently developed at this HTT to cause deflection of the crack along the length of this interphase. With further straining, a single matrix crack is formed that traverses the composite, deflecting around the fibers and bridged by intact fibers (Fig. 6). Additional straining of the composite causes the formation of periodic matrix cracks, which divide the composite into blocks of matrix held together by intact fibers. This is shown in the lower magnification photo of Fig. 7, in which the composite is seen in the center of the photo embedded in the epoxy resin matrix.

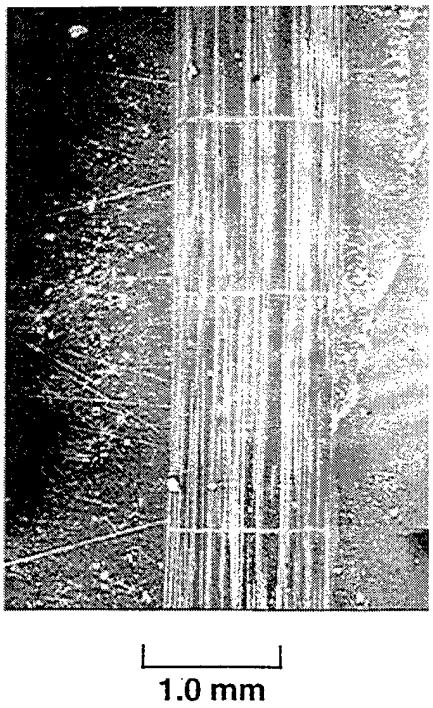

Fig. 7. Multiple matrix cracks formed in 2150°C heat-treated composite.

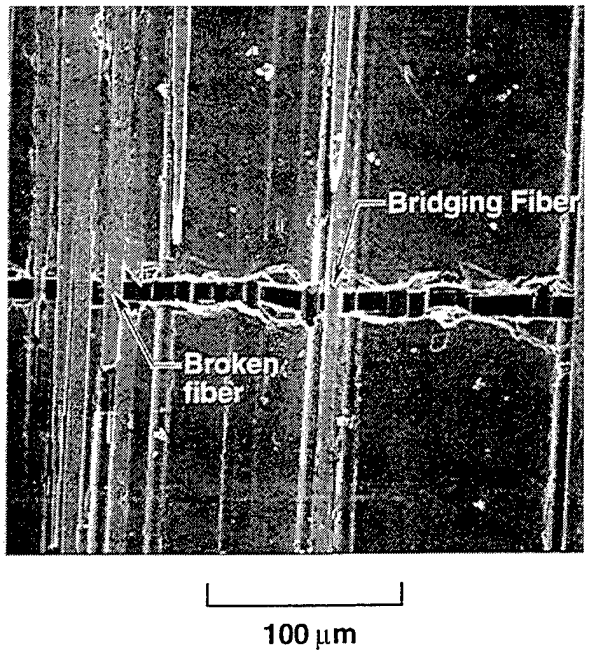

Fig. 8. Matrix slippage over bridging fibers in 2150°C heat-treated composite.

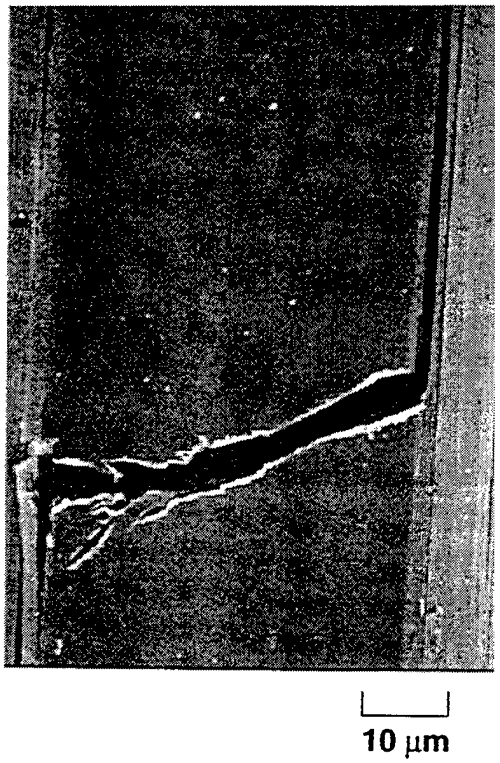

Fig. 10. Short-range longitudinal intramatrix splitting in 2400°C heat-treated composite.

The now-classic theory of Aveston, Cooper, and Kelly (ACK)[24] predicts this phenomenon of multiple matrix cracking in brittle-matrix composites, and argues that it should coincide with the onset of nonlinear behavior in the stress–strain curve. However, in our previous work,[12] in which these same specimens were broken in uniaxial tension, the stress–strain curves were always linear up to failure. Kim and Pagano[25] also failed to observe deviation from linear behavior in their stress–strain curves of fiber-reinforced glass-ceramics even though matrix cracking was observed microscopically and by acoustic emission in the linear region of the curve. However, as pointed out by Yang and Knowles,[26,27] unless a large number of cracks form simultaneously, we should not expect to see a significant deflection of the stress–strain curve. The average spacing of the cracks in the 2150°C HTT sample is about 1 mm, and the crack width is about one fiber diameter at the point where the crack tip has traversed the entire width of the specimen. Increasing the strain on the composite still further causes the matrix blocks to slip over the reinforcing fibers, as shown in Fig. 8, implying that the fiber and matrix are frictionally bonded at this point (i.e., for this HTT). Bridging of the crack by carbon fibers can also be seen in Fig. 8. Some of these fibers are clearly broken. However, we were able to confirm that those fibers that appear intact in the photo were intact along the entire length of the specimen (approximately 2.5 in.). The bridging fibers provide crack-surface-closure tractions, which reduce stresses in the matrix crack tip. The maximum FSU of 92% is attained for the 2150°C HTT composite (Table I), suggesting that the composite has achieved something close to an optimum interfacial shear strength (IFSS), meaning that the bond strength is sufficiently weak so that there is no longer matrix-dominated failure, yet strong enough to effectively utilize the stress-transfer capabilities of the matrix.

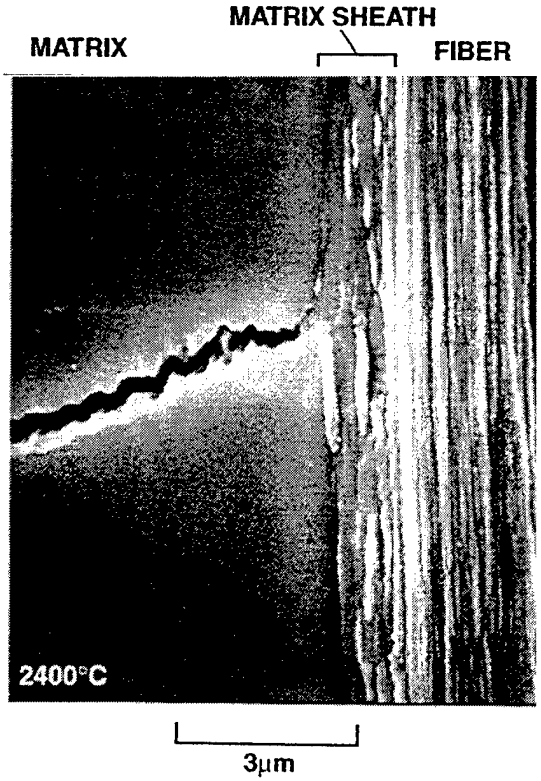

Fig. 9. High-magnification micrograph showing crack blunting at graphitized matrix sheath structure in 2400°C heat-treated composite.

It has been suggested to us by one of the reviewers that the crack-opening displacement seen in Fig. 8 is about 50% of the size of the gaps between the two broken filaments seen on the left of the photo, suggesting significant residual stresses in the fiber; this leads to the question of the role of the epoxy polymer mount in limiting or controlling the damage to the composite. There is little question that the epoxy mount controls the degree of damage, and, in fact, this is one of the reasons for its use. Without it, the cracks would probably move too quickly to follow. But we do not believe the nature of the crack behavior is affected; rather, the mount allows us to gain greater sensitivity and control over what is otherwise a relatively insensitive flexure stage.

With heat treatment to 2400°C, the oriented matrix sheath becomes well graphitized, as evidenced by its lamellar texture,

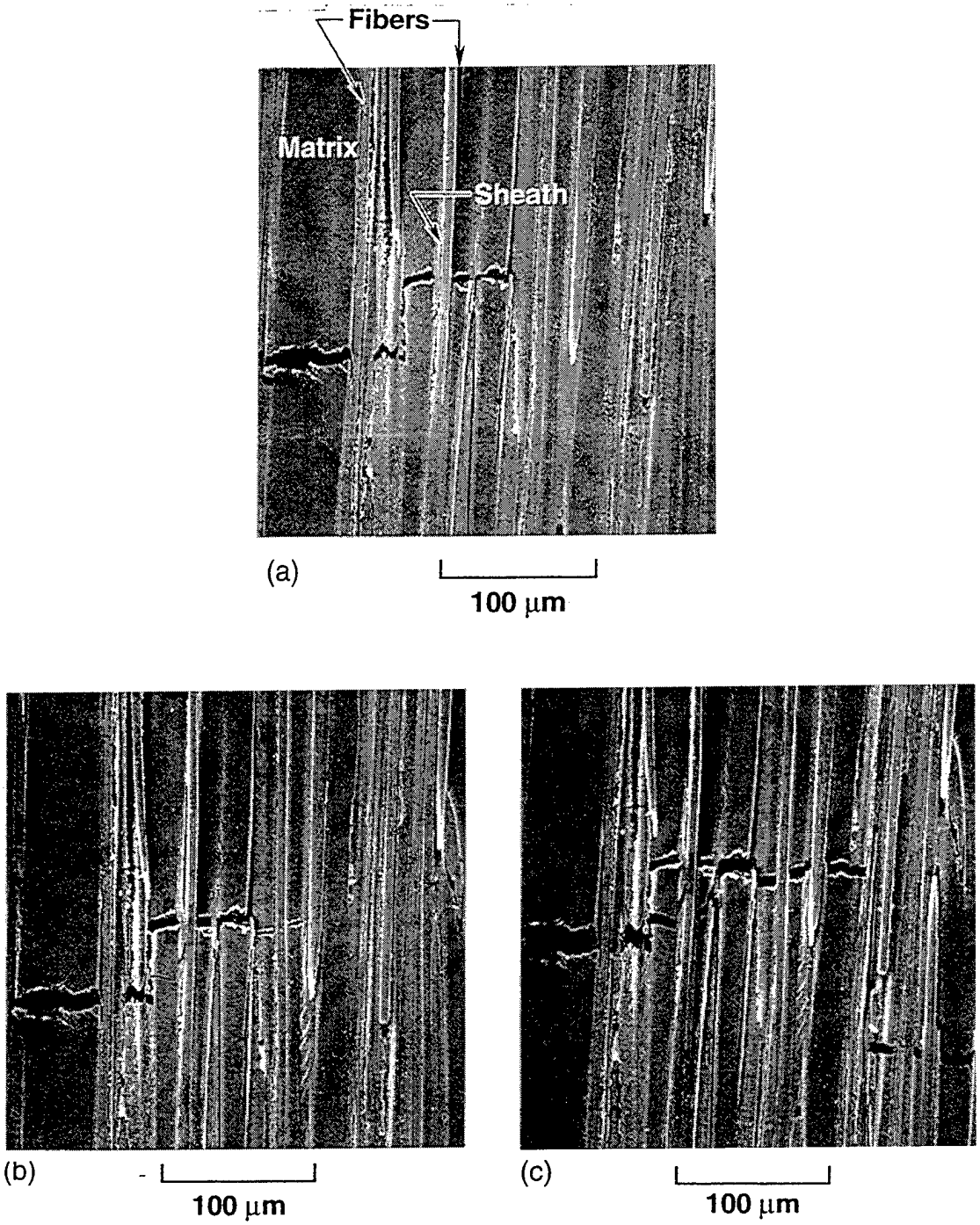

Fig. 11. Crack propagation through a 2400°C heat-treated composite at three levels of strain increasing from (a) to (c). The graphitized sheath appears light gray in the micrographs in comparison to the darker gray less oriented and graphitized matrix regions.

and is almost indistinguishable from the graphitic E130 fiber (Fig. 9; compare to Fig. 5). Crack blunting at the graphitized matrix interphase sheath is also shown in Fig. 9. The high degree of orientation and lamellar graphitic structure of the sheath leads to significant delamination cracking in the sheath along the direction of the filament (Fig. 10). However, this intramatrix cohesive failure also reduces the load-carrying capabilities of the matrix. Figures 11(a–c) show the sequence of crack propagation through the 2400°C HTT sample. Note that the darker gray (and usually thicker) regions are nongraphitized, glassy-carbon-type matrix, whereas the sheath structure appears lighter gray like the fiber for the reasons discussed earlier. The extent of orientation and graphitization of the sheath region varies greatly over the length of the composite. The fracture path through the matrix is significantly more tortuous than for the 2150°C HTT composite. Although some cracks are deflected at the sheath, crack deflection occurs primarily at the interface between graphitized sheath (i.e., interphase) and fiber. Relative to the lower HTT specimens, a much smaller degree of deflection is required to open the crack. By the time the crack has traversed the composite, the crack opening is quite substantial. The development of this well-oriented and graphitized sheath no doubt facilitates the frictional sliding of the fiber. Figure 12 is a higher-magnification view of a crack zone showing well-defined regions of nongraphitized matrix, graphitized matrix sheath, and fiber. Note the extensive debonding between fiber and matrix.

Following the highest HTT of 2750°C, the development of the graphitized sheath interphase is very extensive along the length of the interfacial region. Figures 13(a) and (b) show a

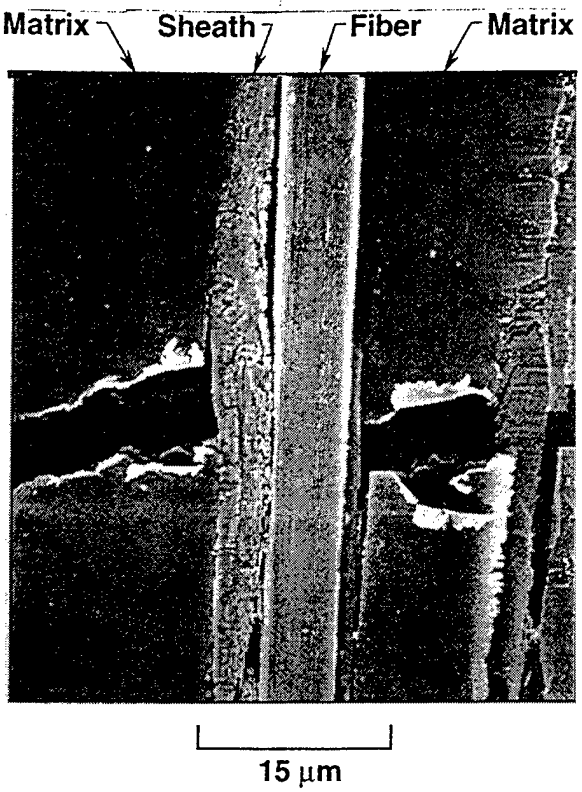

Fig. 12. Crack zone showing well-defined regions of nongraphitized matrix, graphitized sheath, and fiber in 2400°C heat-treated composite.

sequence of two micrographs of the composite as it is strained. As the crack propagates across the width of the composite, it is first deflected around a zone of sheath (left side of Fig. 13(a)). The fiber associated with this sheath has been removed by polishing. The crack then becomes blunted at the fiber F after it passes through a second sheath. Further straining (Fig. 13(b)) leads to partial fracture of the filament F and extensive longitudinal splitting of the matrix sheath region labeled S. Note the saw-toothed structure of the fractured sheath, seen best (better?) in the higher magnification view of Fig. 13(c). At this point, the intramatrix cohesive failure of the sheath is very extensive, leading to a decoupling of the surrounding matrix from the fibers. From Table I we see that the FSU has fallen to its lowest value of 42%. In addition to the very weak coupling between fiber and matrix for this HTT, in the previous study, we also found evidence of fiber degradation resulting from the C/C processing.[12]

IV. Discussion

The predominately brittle fracture observed for the E130 composite/1100°C HTT, although mitigated somewhat by the tough fiber fracture as already discussed, was typical of most of the C/Cs that we have investigated to date. This could suggest very large frictional stresses at the fiber–matrix interface generated as a result of the matrix shrinkage in its conversion from polymer to carbon. We can attempt an estimate of these frictional stresses and then compare them with estimates of interfacial shear debonding stresses associated with an advancing crack using an approach due originally to Cook and Gordon[14] for isotropic solids and extended by Kelly[28] to the case of unidirectional carbon-fiber composites.

The problem that we face here is extremely difficult because so little is known about the thermal degradation and carbonization of polymers, and a number of tenuous assumptions must be made. Nevertheless, we think the problem can be bounded to deal with the particular case at hand. First, we know that the large pyrolysis shrinkage strains of PAA and phenolic resins subjected to 1100°C HTT are about 40% and 45%, respectively.[18] Clearly, these are essentially irreversible strains associated with the conversion of one material (polymer) to another (carbon), and the attendant weight loss occurring roughly over about the same temperature range. It is a reasonable assumption that some significant portion of this volume change occurs nearly stress-free, perhaps associated with some viscous flow. One approximation is to say that the shrinkage is stress-free over that temperature range where the weight loss is the greatest. Based on weight loss and shrinkage for PAA (and phenolic) published previously,[17] we would estimate 700°C as the end of the major weight-loss regime, and, therefore, the stress-free temperature.

Next, we note that Jenkins and Leaves[29] have measured Young's modulus of pyrolyzed phenolic resin for HTTs of 450° to 1200°C, and report values of 2 and 28 GPa for these two respective HTTs. In their experiment, the modulus is not an *in situ* value, but rather is obtained on specimens cooled to room temperature. However, based on the work of Andrew and Sato,[30] we know that, for glassy carbon structures such as the pyrolyzed phenolic resin, there is little effect of temperature on modulus from room temperature to about 1000°C. Therefore, Jenkins and Leaves' values should represent reasonable approximations to *in situ* values. We are using phenolic resin properties in lieu of any comparable data for PAA; however, our studies of the pyrolysis products of the two resins strongly suggest they are very similar in structure and properties.[19,20]

The approach to the shrinkage of the matrix is to treat it as elastic over the temperature range 700° to 1100°C (6%[17]), although it is clear that the shrinkage is irreversible in the mechanical sense and is associated with densification of the carbon. To distinguish it from a free thermal strain, we term it a transformation strain, ε_t.

For the fiber, we are interested in its transverse properties, i.e., the properties in the direction transverse to the fiber axis. Relative to the axial properties, these are known only approximately. Using the compilation of fiber properties in Dresselhaus *et al.*,[31] we assign for the E130 fiber $E_f^t = 7$ GPa, $\alpha_f^t = 10^{-5}$ °C^{-1}. For a fiber diameter of 10 μm,[12] we obtain a fiber volume fraction of 0.25 if the matrix thickness is 5 μm (i.e., the radius of the cylindrical fiber and matrix together is 10 μm).

Details of the calculation are given in the Appendix. For a −6% linear transformation strain, ε_t, in the matrix, and using the upper limit of matrix modulus of 28 GPa, we obtain a radial compressive stress of 400 MPa. Using a coefficient of friction of 0.3,[32,33] to obtain an interfacial shear stress (IFSS), we calculate an IFSS of 120 MPa (the cooldown stresses are negligible).

Next, we are interested in comparing the IFSS with the stresses acting on the interface as the matrix crack propagates through the composite in a direction perpendicular to the fibers. As discussed first by Cook and Gordon,[14] in addition to the major crack-opening stress σ_y, which acts in the direction of applied tensile load, i.e., parallel to the fiber, there is also a stress σ_x at the crack tip which is perpendicular to σ_y, i.e., parallel to the length of the crack and perpendicular to the length of the fiber. Cook and Gordon deal with an elliptically shaped crack of 0.1-nm tip radius and 2 μm long. The stress σ_x has the effect of being able to produce an interface crack that could deflect the main crack. Cook and Gordon found that the maximum value of σ_x was an approximately constant fraction (~1/5) of the peak stress concentration σ_y.

Kelly[28] cites the analyses of a number of workers who have made similar calculations for the case of elastic anisotropy appropriate to an aligned fibrous composite. For the particular case of a carbon/epoxy composite with 50% fibers by volume, it was found that the crack deflecting stress σ_x is greatly reduced in the composite; e.g., $\sigma_y^{max}/\sigma_x^{max}$ is now 47 compared to 5 for the isotropic case. However, the value of the shear stress parallel to the fibers τ_{xy} is larger than σ_x^{max} by a factor of 4.4. Based on these findings, Kelly indicates that we should always expect interfacial shear failure to dominate the composite failure mode.

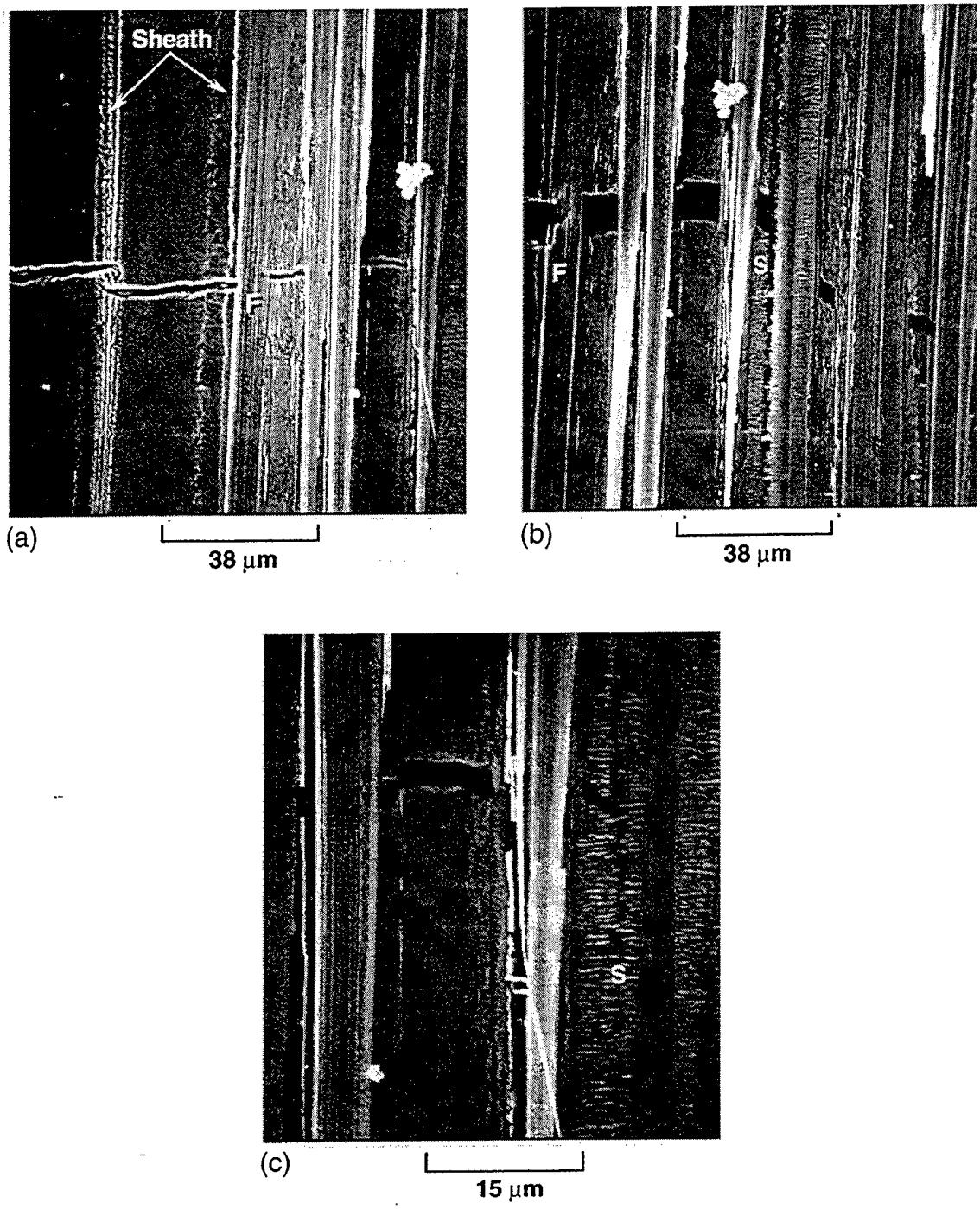

Fig. 13. Crack propagation through a 2750°C heat-treated composite at two different degrees of strain, (a) and (b); (c) is a higher magnification view of (b) at a slightly lower degree of strain.

In our C/Cs heated to 1100°C, this is clearly not the case, as the mode of fracture is brittle; it is interesting to see if we can use Kelly's arguments to estimate τ_{xy} and compare it with our estimated matrix-shrinkage-induced frictional IFSS. First, we note that σ_y^{max} must be at least as large as the E130 fiber strength of 2.7 GPa (using the manufacturer's reported single-filament data), since the advancing crack breaks the fibers. But rather than restrict our analysis to the E130 fiber, we take note that brittle, monolithic-like fracture has also been seen by us in ultra-high-strength, PAN-based IM6 fibers having tensile strengths of about 5 GPa.[34] So we use 5 GPa as a lower limit for σ_y^{max} and select a more conservative value of 20 for $\sigma_y^{max}/\sigma_x^{max}$, relative to Kelly's 47 for the higher volume fraction graphite/epoxy composite, and use the same ratio of τ_{xy}/σ_x^{max} of 4.4; this gives us a crack tip shear stress of (4.4)(5/20) = 1.1 GPa. This is about an order of magnitude greater than the 120 MPa frictional IFSS, which we calculated and which we believe to be an upper bound estimate because of the use of linear elastic theory. While there is a good deal of uncertainty in all of these numbers, nevertheless, we are led to the conclusion that simple frictional bonding between fiber and matrix almost certainly cannot account for the brittle fracture of the 1100°C HTT unidirectionals, and, therefore, either chemical bonding or, more likely, we believe, based on our other work,[34] some type of mechanical interlocking between fiber and matrix must be involved.

Another important feature of the present work is the transition from brittle fracture for the 1100°C HTT to multiple matrix cracking (MMC) at the HTT of 2150°C. Clearly the interface has been weakened by the large thermal stresses associated

with heatup and cooldown from these high HTTs, as well as by the formation of the well-oriented, graphitized interphase, a subject that we have discussed in detail elsewhere.[19,20] As Fig. 7 reveals, MMC occurs in the 2150°C HTT sample at some point prior to fiber failure. The average spacing of the cracks is about 1 mm. According to Aveston, Cooper, and Kelly,[24] the limiting crack separation in a brittle-matrix composite is between x' and $2x'$ where

$$x' = \frac{V_m}{V_f}\cdot\sigma_{mu}\frac{r}{2\tau_i} \tag{1}$$

and where V_m and V_f are matrix and fiber volume fractions, σ_{mu} is the strength of the unreinforced matrix, r is the fiber radius, and τ_i is the interfacial shear strength. For a mean crack spacing s, ACK show that $s = 1.36x'$. The big problem with calculating τ_i is the uncertainty in σ_{mu}. Recall that this matrix is formed *in situ* and we can only infer its properties from composite properties. One piece of information available to us is that the matrix contributes negligibly to the modulus of the composite for this HTT.[12] If we assume very liberally that this "negligible" contribution could be as high as 15%, then using rule of mixtures and fiber and matrix volume fractions of 0.30 and 0.70, we calculate an upper bound for the matrix modulus to be roughly 50 GPa. It is also of some interest to attempt a calculation of the reinforced-matrix cracking stress (or strain) for this particular composite using the ACK approach, which states that the strain at which the reinforced matrix first cracks is given by

$$\varepsilon_{muc} = \left[\frac{12\tau_i\gamma_m V_f^2 E_f(1-\nu^2)^2}{rV_M E_c E_M^2}\right]^{1/3} \tag{2}$$

We can solve this by solving Eq. (1) for τ_i and then substituting the expression for it into Eq. (2). We further state that σ_{mu} = 50 GPa × ε_{muc}, leaving ε_{muc} as the only variable for which to solve.

In addition to the terms already identified (see Appendix), we use 200 J/m^2 for the fracture energy γ_m of the carbon matrix.[36] From this, we calculate a matrix failure strain of ~0.5%, which is well above that observed for the composite (~0.2–0.25%). Clearly, this calculation is very approximate because of large uncertainties of E_m, E_c, and γ_m. However, it is interesting to note that Kim and Pagano,[25] working with a number of ceramic-matrix composites, similarly calculate failure strains using ACK that are much higher than those measured.

We can also estimate the IFSS τ_i from Eq. (1) based on the measured multiple matrix crack spacing of 1 mm and using the experimentally observed composite failure strain of ~0.2% and the matrix modulus of 50 GPa (giving $\sigma_{mu} \cong$ 100 MPa). We then calculate τ_i to be on the order of only 1 MPa, which is quite a bit lower than the values reported for a number of ceramic-matrix composites.[35]

V. Conclusions

The three distinct failure regimes of E130/PAA-derived C/C composites can be summarized as follows. After carbonization heat treatment (1100°C), the composite strength is dominated by the low strain-to-failure of the matrix as well as by the nonbrittle fiber fracture mode. In the second regime (1600°C), heat treatment weakens the interface, thereby reducing the likelihood of matrix-dominated failure. This allows fiber bridging across matrix cracks and contributes to crack-tip shielding by the filaments. However, there are still well-bonded regions that result in brittle crack propagation. The result is a mixed-mode type of failure. With heat treatment to 2150°C, multiple matrix cracking is observed, with intact fibers bridging the cracks. The onset of matrix interphase (sheath) structure development is also first evident at this HTT. This sheath microstructure at the 2150°C HTT is seen in one instance to cause blunting of the crack but no deflection of the crack along the sheath length. Something approaching an optimum strength utilization is realized for the 2150°C HTT, based on previous uniaxial tensile tests.[12] Heat treatment above this temperature (2400° and 2750°C) leads to longitudinal intramatrix cohesive failure caused by the weakness of the highly oriented and graphitized matrix sheath, which causes long-range deflection along the weakly bonded graphite planes that are aligned parallel to the fibers. For the 2750°C HTT, the result is composites with strength utilizations approaching those of dry fiber bundles. Calculations of the interfacial shear stress that might be generated by matrix shrinkage during pyrolysis of the polymer to carbon were made using a simplified model. These results were compared to approximations of crack-tip interfacial shear stresses (IFSS) using the Cook–Gordon crack deflection model. The results suggest that the strong bonding in the 1100°C HTT composite cannot be accounted for by friction alone, and, therefore, chemical bonding or some type of fiber–matrix mechanical interlocking must be involved. Using the crack-spacing model of Aveston, Cooper, and Kelly (ACK) an IFSS of ~1 MPa is estimated for the MMC case corresponding to the 2150°C HTT. Attempts to calculate the matrix failure strain using the ACK formulation led to a large overprediction of the failure strain, although a number of the parameters used in the calculation are known only very approximately.

APPENDIX

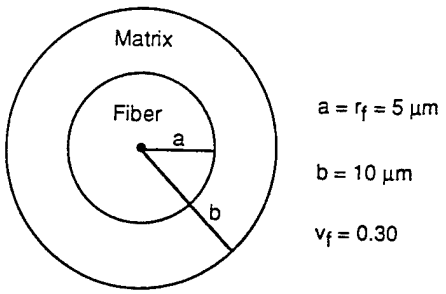

For the above fiber–matrix configuration, we calculate the thermal stresses due to matrix shrinkage on heatup. We use the equations of stress states of a solid rod and a hollow cylinder subject to normal pressure (external for rod and internal for cylinder) as outlined in Timoshenkso and Goodier.[37] From our discussion in the text, we use

$\varepsilon_t = -0.06$

E_m = 28 GPa

$\alpha_f = 10^{-5}$ °C^{-1} (transverse)

E_f = 7 GPa (transverse)

ΔT = 400°C

ν (Poisson ratio) = 0.3 (for both fiber and matrix)

The thermally induced mismatch in radial displacement for the stress-free state at the fiber–matrix interface $r = a$ is given by

$$\alpha_f\, a\Delta T - \varepsilon_t a \tag{A-1}$$

To eliminate this displacement mismatch, a mechanical normal stress, P, is applied at the interface. The radial displacements for the fiber and matrix, Δr_f and Δr_m, are

$$\Delta r_f = \frac{-Pa}{E_f}(1-\nu) \tag{A-2}$$

$$\Delta r_m = \frac{P}{E_m}\frac{a}{(b^2-a^2)}\left[(1+\nu)b^2 + (1-\nu)a\right] \tag{A-3}$$

The equation for displacement compatibility at the fiber–matrix interface is

$$(\Delta r_f - \Delta r_m) - (\alpha_f a \Delta T - \varepsilon_t a) = 0 \qquad \text{(A-4)}$$

Combining Eqs. (2), (3), and (4), and solving for P, yields the value of 400 MPa. We estimated the cooldown stresses using the same fiber α_f but a stabilized matrix α_m of 3×10^{-6} °C^{-1}.[38] This had the effect of reducing the radial stress by only about 10%.

Acknowledgment: We would like to thank Dr. Dick Chang for his assistance with the mechanics calculations.

References

[1]For a review, see: A. G. Evans, "Perspective on the Development of High Toughness Ceramics," *J. Am. Ceram. Soc.*, **73** [2] 187–206 (1990).

[2]E. Fitzer and Burger, "The Formation of Carbon/Carbon Composites by Thermally Decomposing Carbon-Fibre-Reinforced Thermosetting Polymers"; pp. 134–41 in *Carbon Fibers: Their Composites and Applications*. The Plastics Institute. London, U.K.. 1971.

[3]D. O. Newling and E. J. Walker, "High Performance Graphitized Carbon/Carbon Composites"; pp. 142–53 in *Carbon Fibers: Their Composites and Applications*. The Plastics Institute, London, U.K., 1971.

[4]E. Fitzer, K. H. Geigl, and W. Huttner, "The Influence of Carbon Fibre Surface Treatment on the Mechanical Properties of Carbon/Carbon Composites," *Carbon*, **18** [4] 265–70 (1980).

[5]E. Fitzer, W. Huttner, and L. M. Manocha, "Influence of Process Parameters on the Mechanical Properties of Carbon/Carbon Composites with Pitch as Matrix Precursor," *Carbon*, **18** [4] 291–95 (1980).

[6]J. Jortner, "Microstructure of Cloth-Reinforced Carbon–Carbon Laminates," *Carbon*, **30** [2] 153–63 (1992).

[7]J. Jortner, "Effects of Crimp Angle on the Tensile Strength of a Carbon–Carbon Laminate"; pp. 243–51 in *Symposium on High Temperature Composites*, Proceedings of the American Society for Composites. Technomic Publishing, Lancaster, PA, 1989.

[8]P. B. Pollock, "Tensile Failure in 2-D Carbon–Carbon Composites," *Carbon*, **28**, 717–32 (1990).

[9]A. Moet, I. Mostafa, A. Chudnovsky, and B. Kunin, "Probabilistic Fracture Mechanics of 2D Carbon–Carbon Composites," *Int. J. Fract.*, **55**, 179–91 (1992).

[10]S. Senet, R. E. Grimes, D. L. Hunn, and K. W. White, "Elevated Temperature Fracture Behavior of a 2-D Discontinuous Fiber Reinforced Carbon/Carbon Composites," *Carbon*, **29** [7] 1039-49 (1991).

[11]F. E. Heredia, S. M. Spearing, A. G. Evans, P. Mosher, and W. A. Curtin, "Mechanical Properties of Continuous-Fiber-Reinforced Carbon Matrix Composites and Relationships to Constituent Properties," *J. Am. Ceram. Soc.*, **75** [11] 3017–25 (1992).

[12]R. J. Zaldivar, G. S. Rellick, and J. M. Yang, "Fiber Strength Utilization in Carbon/Carbon Composites," *J. Mater. Res.*, **8** [3] 501–11 (1993).

[13]C. R. Thomas and E. J. Walker, "Carbon–Carbon Composites as High Strength Refractories," *High Temp–High Pressures*, **10**, 79–86 (1978).

[14]J. Cook and J. E. Gordon, "A Mechanism for Control of Crack Propagation in All-Brittle Systems," *Proc. R. Soc. London*, **A282**, 508–20 (1964).

[15]G. S. Rellick and P. M. Adams, "TEM Studies of Resin Based Matrix Microstructure in Carbon/Carbon Composites," *Carbon*, **32** [1] 127–44 (1994).

[16]R. J. Zaldivar, G. S. Rellick, and J. M. Yang, "Processing Effects on the Mechanical Behavior of Polyarlacetylene-Derived Carbon–Carbon Composites," *SAMPE J.*, **27**, 29–36 (1991).

[17]R. J. Zaldivar, R. W. Kobayashi, G. S. Rellick, and J. M. Yang, "Carborane-Catalyzed Graphitization in Polyarylacetylene-Derived Carbon–Carbon Composites," *Carbon*, **29** [8] 1145–53 (1991).

[18]G. S. Rellick and R. J. Zaldivar, "*In Situ* Matrix Properties in Unidirectional Carbon/Carbon Composites," *Ext. Abstr. Program–Bienn. Conf. Carbon*, **21**, 68–69 (1993).

[19]R. J. Zaldivar and G. S. Rellick, "Some Observations on Stress Graphitization in Carbon–Carbon Composites," *Carbon*, **29** [8] 1155–63 (1991).

[20]G. S. Rellick, D. J. Chang, and R. J. Zaldivar, "Mechanisms of Orientation and Graphitization of Hard-Carbon Matrices in Carbon/Carbon Composites," *J. Mater. Res.*, **7** [10] 2798–809 (1992).

[21]D. B. Marshall and A. G. Evans, "Failure Mechanisms in Ceramic-Fiber/Ceramic-Matrix Composites," *J. Am. Ceram. Soc.*, **68** [5] 225–31 (1985).

[22]D. Edie, R. J. Cano, and R. A. Ross, "Observing Fiber Surface Treatments by Dynamic Analysis," *Ext. Abstr. Program–Bienn. Conf. Carbon*, **20**, 330–31 (1991).

[23]J. S. Evangelides, "Influence of Pyrolysis Pressure on Microstructure of Carbon–Carbon Composites," *Ext. Abstr. Program–Bienn. Conf. Carbon*, **13**, 76–77 (1977).

[24]J. Aveston, G. Cooper, and A. Kelly, "Single and Multiple Fracture"; pp. 15–26 in *The Properties of Fiber Composites* (Conference Proceedings of the National Physical Laboratory, Teddington, U.K.). IPC Science and Technology Press, Guildford, U.K., 1971.

[25]R. Y. Kim and N. J. Pagano, "Crack Initiation in Unidirectional Brittle-Matrix Composites," *J. Am. Ceram. Soc.*, **74** [5] 1082-90 (1991).

[26]X. F. Yang and K. M. Knowles, "The One-Dimensional Car Parking Problem and Its Application to Matrix Cracks in Fiber-Reinforced Brittle Materials," *J. Am. Ceram. Soc.*, **75** [1] 141–17 (1992).

[27]X. F. Yang and K. M. Knowles, "On the First-Matrix-Cracking Stress in Unidirectional Fiber Reinforced Brittle Materials," *J. Mater. Res.*, **8** [2] 371–76 (1993).

[28]A. Kelly, "Interface Effects and the Work of Fracture of a Fibrous Composite," *Proc. R. Soc. London*, **A319**, 95–116 (1981).

[29]G. Jenkins and M. Leaves, "Plastic Behavior of Phenolic Resin Thermosets Immediately Prior to Carbonization," *Ext. Abstr. Program–Bienn. Conf. Carbon*, **15**, 160–61 (1981).

[30]J. F. Andrew and S. Sato, "Studies of Young's Modulus of Carbons at High Temperature," *Carbon*, **1** [2] 225–34 (1964).

[31]M. S. Dresselhaus, G. Dresselhaus, K. Sugihara, I. L. Spain, and H. A. Goldberg, *Graphite Fibers and Filaments*. Springer-Verlag, Berlin, Germany, 1988.

[32]R. Taylor, R. Brown, K. E. Gilchrist, A. T. Hodds, B. T. Kelly, F. Morris, and E. Hall, "The Mechanical Properties of Reactor Graphite," *Carbon*, **5**, 519–31 (1967).

[33]S. Awasthi and J. C. Wood, "C/C Composites Materials for Aircraft Brakes," *Adv. Ceram. Mater.*, **3** [5] 449–51 (1988).

[34]R. J. Zaldivar, G. S. Rellick, and J. M. Yang, *J. Mater. Res.*, in press.

[35]B. Harris, F. A. Habib, and R. G. Cooke, "Matrix Cracking and the Mechanical Behavior of SiC–CAS Composites," *Proc. R. Soc. London*, **A437**, 109–31 (1992).

[36]J. F. Brocklehurst, "Fracture in Polycrystalline Graphite"; pp. 145–279 in *Chemistry and Physics of Carbon*, Vol. 13. Edited by P. L. Walker, Jr., and P. A. Thrower. Marcel Dekker, New York, 1977.

[37]S. Timoshenkso and J. N. Goodier, *Theory of Elasticity*; pp. 58–60. McGraw-Hill, New York, 1951.

[38]G. M. Jenkins and R. A. Jones, "A Dilatometric Study of the Carbonization of Phenolic Resin," *High Temp.–High Pressures*, **9**, 137–44 (1977). □

TECHNOLOGY OPERATIONS

The Aerospace Corporation functions as an "architect-engineer" for national security programs, specializing in advanced military space systems. The Corporation's Technology Operations supports the effective and timely development and operation of national security systems through scientific research and the application of advanced technology. Vital to the success of the Corporation is the technical staff's wide-ranging expertise and its ability to stay abreast of new technological developments and program support issues associated with rapidly evolving space systems. Contributing capabilities are provided by these individual Technology Centers:

Electronics Technology Center: Microelectronics, VLSI reliability, failure analysis, solid-state device physics, compound semiconductors, radiation effects, infrared and CCD detector devices, Micro-Electro-Mechanical Systems (MEMS), and data storage and display technologies; lasers and electro-optics, solid state laser design, micro-optics, optical communications, and fiber optic sensors; atomic frequency standards, applied laser spectroscopy, laser chemistry, atmospheric propagation and beam control, LIDAR/LADAR remote sensing; solar cell and array testing and evaluation, battery electrochemistry, battery testing and evaluation.

Mechanics and Materials Technology Center: Evaluation and characterization of new materials: metals, alloys, ceramics, polymers and composites; development and analysis of advanced materials processing and deposition techniques; nondestructive evaluation, component failure analysis and reliability; fracture mechanics and stress corrosion; analysis and evaluation of materials at cryogenic and elevated temperatures; launch vehicle fluid mechanics, heat transfer and flight dynamics; aerothermodynamics; chemical and electric propulsion; environmental chemistry; combustion processes; spacecraft structural mechanics, space environment effects on materials, hardening and vulnerability assessment; contamination, thermal and structural control; lubrication and surface phenomena; microengineering technology and microinstrument development.

Space and Environment Technology Center: Magnetospheric, auroral and cosmic ray physics, wave-particle interactions, magnetospheric plasma waves; atmospheric and ionospheric physics, density and composition of the upper atmosphere, remote sensing, hyperspectral imagery; solar physics, infrared astronomy, infrared signature analysis; effects of solar activity, magnetic storms and nuclear explosions on the earth's atmosphere, ionosphere and magnetosphere; effects of electromagnetic and particulate radiations on space systems; component testing, space instrumentation; environmental monitoring, trace detection; atmospheric chemical reactions, atmospheric optics, light scattering, state-specific chemical reactions and radiative signatures of missile plumes, and sensor out-of-field-of-view rejection.